

Structural Investigation and Photoluminescent Properties of Gadolinium(III), Europium(III) and Terbium(III) 3-Mercaptopropionate Complexes

E. R. Souza · I. O. Mazali · F. A. Sigoli

Received: 10 July 2013 / Accepted: 9 August 2013 / Published online: 18 August 2013
© Springer Science+Business Media New York 2013

Abstract This work reports on the synthesis, crystallographic determination and spectroscopic characterization of gadolinium(III), terbium(III) and europium(III) 3-mercaptopropionate complexes, aqua-tris(3-mercaptopropionate) lanthanide(III) - $[\text{Ln}(\text{mpa})_3(\text{H}_2\text{O})]$. The Judd-Ofelt intensity parameters were experimentally determined from emission spectrum of the $[\text{Eu}(\text{mpa})_3(\text{H}_2\text{O})]$ complex and they were also calculated from crystallographic data. The complexes are coordination polymers, where the units of each complex are linked together by carboxylate groups leading to an unidimensional and parallel chains that by chemical interactions form a tridimensional framework. The emission spectrum profile of the $[\text{Eu}(\text{mpa})_3(\text{H}_2\text{O})]$ complex is discussed based on point symmetry of the europium(III) ion, that explains the bands splitting observed in its emission spectrum. Photoluminescent analysis of the $[\text{Gd}(\text{mpa})_3(\text{H}_2\text{O})]$ complex show no efficient ligand excitation but an intense charge transfer band. The excitation spectra of the $[\text{Eu}(\text{mpa})_3(\text{H}_2\text{O})]$ and $[\text{Tb}(\text{mpa})_3(\text{H}_2\text{O})]$ complexes do not show evidence of energy transfer from the ligand to the excited levels of these trivalent ions. Therefore the emission bands are originated only by direct $f-f$ intraconfigurational excitation of the lanthanide(III) ions.

Keywords Luminescence · Lanthanide · 3-mercaptopropionate

Introduction

Coordination polymers consist on spatial structures formed by metal ions and ligands where the unities of the complex are bonded forming chains in one, two or three dimensions [1, 2]. This class of compounds has a wide possibility of spatial organization [3, 4]. Some coordination polymers form porous structures allowing them to be applicable in many areas, such as gas purification and separation [5–7], drugs storage [8], heterogeneous catalysis [9] etc.

Metal ions in coordination polymers have been studied and developed due to their wide applications such as gas storage, insertion of other molecules in the structure lattices [10]. Their spatial structures can be extended in one (1D), two (2D) or three dimensions(3D). To build these kinds of structures it is common to use multidentate ligands, for example carboxylates. The carboxylate group may present many coordination modes, from mono to tridentate [11], and that is one of the reasons because the carboxylate ligands are widely used in building inorganic frameworks. The ligand 3-mercaptopropionic acid (Hmpa), is often used as surface stabilizer of metal nanoparticles [12, 13] and quantum dots [14, 15]. As nucleophile, the sulfur atom of the Hmpa may interfere in photochemistry of other complexes such as iron(II) complexes [16] or act as reducing agent [17, 18]. For instance, Su et al. [19] used Hmpa combined to DNA-Cu/Ag nanoclusters to detect Cu(II) ions by fluorescence quenching. Also in the biological field, Prasad et al. [20] observed that the Schiff base oxovanadium(IV) complexes of phenanthroline bases does not show DNA photocleavage activity anymore in presence of 3-mercaptopropionic acid (added as reducing agent), due to the poor redox activity oxovanadium(IV) complexes showing quasi-reversible

CCDC 883721 contains the supplementary crystallographic data for this paper. These data can be obtained free of charge from The Cambridge Crystallographic Data Centre via www.ccdc.cam.ac.uk/data_request/cif.

Electronic supplementary material The online version of this article (doi:10.1007/s10895-013-1288-5) contains supplementary material, which is available to authorized users.

E. R. Souza · I. O. Mazali · F. A. Sigoli (✉)
Laboratory of Functional Materials - Institute of Chemistry,
University of Campinas - UNICAMP, Campinas, SP 13083-970,
Brazil
e-mail: fsigoli@iqm.unicamp.br

V(IV)–V(III) redox processes near -0.6 V. Most of the reports about the use of 3-mercaptopropionic acid on coordination compounds are related to transition metal ions.

Specifically about lanthanide(III) complexes with mercaptopropionate ligand, Bear et. al. [21] determined the stability constants in aqueous solution for many lanthanide 2- and 3-mercaptopropionate complexes, concluding that the ligands act as monodentate. Later Choppin and Martinez-Perez [22] corrected the chemical stability values obtained previously and measured the complexation enthalpy and entropy energies (ΔH , ΔS) of the 2- and 3-mercaptopropionate ligand with the trivalent lanthanide ions. It is important to state that these measurements concerns on the coordination of only one ligand to an aqueous lanthanide trivalent ion.

However, considering the best of our knowledge there is no description about the crystal structure and photoluminescent properties of the lanthanides(III)-based 3-mercaptopropionate complexes. Therefore, this work describes the crystalline structure of three isomorphous one tridimensional lanthanide coordination polymers using 3-mercaptopropionate acid as ligand (Fig. 1). The structural and photoluminescent properties of gadolinium(III), terbium(III) and europium(III) complexes will be shown and discussed.

Experimental Details

The lanthanides oxides were purchased from Aldrich and used without further purification. The lanthanides(III) chloride (LnCl_3) were prepared by dissolving Eu_2O_3 , Gd_2O_3 and Tb_4O_7 in HCl. The excess of acid was eliminated by evaporation and the LnCl_3 were dried under vacuum into a desiccator. Then $3 \cdot 10^{-3}$ mol of Hmpa were added to 5 mL of water containing $3 \cdot 10^{-3}$ mol of NaOH in order to neutralize de acid. After solubilization $1 \cdot 10^{-3}$ mol of RECl_3 in 5 mL of water was added under stirring. The solutions were maintained under stirring for 1 hour and then left to evaporate. After 1 week the crystals of the complexes were filtered off, washed using cold water and kept under vacuum into a desiccator. The thermogravimetric analyses were obtained using a TA SDT Q600 from 27 °C up to 900 °C with 10 °C/min as a heating rate under a synthetic air flow of 100 mL/min. The Fourier transform infrared spectra (FT-IR) were carried out with a Bomem MB – Series model B 100 FTIR spectrometer, with a resolution equal to 4 cm^{-1} and 32 scans per spectrum, in KBr

Fig. 1 Molecular structure of the Hmpa ligand

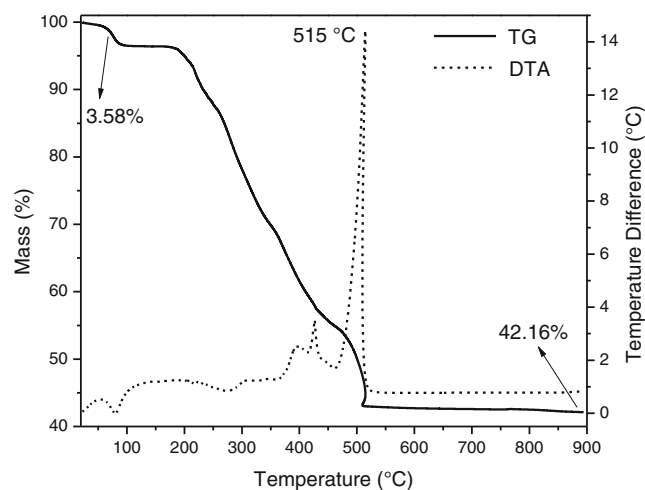
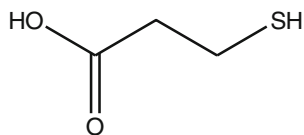


Fig. 2 TG/DTA of the $[\text{Eu}(\text{mpa})_3(\text{H}_2\text{O})]$ complex. The data were obtained between 27 °C and 900 °C under synthetic air dynamic atmosphere

pellets. The photoluminescence data were obtained in a Fluorolog-3 spectrofluorometer (Horiba FL3-22-iHR320),

Table 1 Crystal data and structures for $[\text{Eu}(\text{mpa})_3(\text{H}_2\text{O})]$ complex

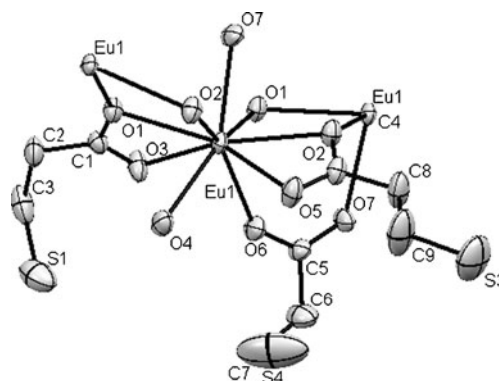
$\text{C}_9\text{H}_{14}\text{EuO}_7\text{S}_3$	$Z=8$
$M_r=482.34$	$F(000)=1880$
Orthorhombic, <i>Pbca</i>	$D_x=1.950 \text{ Mg m}^{-3}$
Hall symbol: -P 2 ac2ab	Mo <i>K</i> α radiation, $\lambda=0.71073 \text{ \AA}$
$a=12.2866 (5) \text{ \AA}$	$\mu=4.22 \text{ mm}^{-1}$
$b=7.7334 (3) \text{ \AA}$	$T=296 \text{ K}$
$c=34.5819 (15) \text{ \AA}$	colourless
$V=3285.9 (2) \text{ \AA}^3$	$0.95 \times 0.16 \times 0.14 \text{ mm}$
Radiation source: fine-focus sealed tube	$R_{\text{int}}=0.034$
Graphite	$\theta_{\text{max}}=27.9^\circ$, $\theta_{\text{min}}=1.2^\circ$
47527 measured reflections	$h=-15 \rightarrow 16$
3912 independent reflections	$k=-9 \rightarrow 10$
3463 reflections with $I > 2\sigma(I)$	$l=-16 \rightarrow 45$
Refinement on F^2	Primary atom site location: structure-invariant direct methods
Least-squares matrix: full	Secondary atom site location: difference Fourier map
$R[F^2 > 2\sigma(F^2)]=0.038$	Hydrogen site location: inferred from neighbouring sites
$wR(F^2)=0.081$	H atoms treated by a mixture of independent and constrained refinement
$S=1.24$	$w=1/[\sigma^2(F_o^2)+(0.P)^2+25.5935P]$ where $P=(F_o^2+2F_c^2)/3$
3912 reflections	$(\Delta\sigma)_{\text{max}}=0.008$
189 parameters	$\Delta_{\text{max}}=1.14 \text{ e \AA}^{-3}$
0 restraints	$\Delta_{\text{min}}=-2.31 \text{ e \AA}^{-3}$

Table 2 Distances between europium(III) ion and surrounding oxygen atoms in the [Eu(mpa)₃(H₂O)] complex

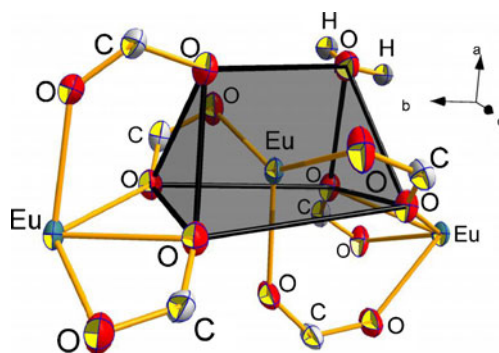
Bond	Distance (Å)
Eu1—O6	2.365 (4)
Eu1—O1 ⁱ	2.393 (4)
Eu1—O7	2.444 (4)
Eu1—O2 ⁱⁱ	2.463 (4)
Eu1—O3	2.468 (4)
Eu1—O4	2.470 (4)
Eu1—O1	2.488 (3)
Eu1—O5	2.509 (4)
Eu1—O2	2.513 (4)

Table 3 Angles between Eu³⁺ ion and surrounding oxygen atoms in the [Eu(mpa)₃(H₂O)] complex

Atoms	Angle (°)
O6—Eu1—O1 ⁱ	73.81 (13)
O6—Eu1—O7	142.20 (13)
O1 ⁱ —Eu1—O7	71.83 (13)
O6—Eu1—O2 ⁱⁱ	139.32 (14)
O1 ⁱ —Eu1—O2 ⁱⁱ	144.18 (14)
O7—Eu1—O2 ⁱⁱ	72.40 (14)
O6—Eu1—O3	76.82 (14)
O1 ⁱ —Eu1—O3	76.29 (13)
O7—Eu1—O3	109.30 (15)
O2 ⁱⁱ —Eu1—O3	117.73 (12)
O6—Eu1—O4	77.54 (14)
O1 ⁱ —Eu1—O4	143.17 (14)
O7—Eu1—O4	140.23 (14)
O2 ⁱⁱ —Eu1—O4	71.17 (15)
O3—Eu1—O4	75.01 (15)
O6—Eu1—O1	125.42 (13)
O1 ⁱ —Eu1—O1	106.49 (12)
O7—Eu1—O1	79.82 (12)
O2 ⁱⁱ —Eu1—O1	68.42 (11)
O3—Eu1—O1	52.05 (12)
O4—Eu1—O1	72.46 (14)
O6—Eu1—O5	73.47 (14)
O1 ⁱ —Eu1—O5	117.38 (12)
O7—Eu1—O5	109.43 (14)
O2 ⁱⁱ —Eu1—O5	73.70 (13)
O3—Eu1—O5	141.25 (15)
O4—Eu1—O5	74.75 (14)
O1—Eu1—O5	135.96 (12)
O6—Eu1—O2	75.10 (14)
O1 ⁱ —Eu1—O2	69.08 (11)
O7—Eu1—O2	78.34 (13)
O2 ⁱⁱ —Eu1—O2	101.99 (11)
O3—Eu1—O2	140.13 (12)
O4—Eu1—O2	124.57 (14)
O1—Eu1—O2	157.98 (13)
O5—Eu1—O2	51.62 (12)

**Fig. 3** ORTEP diagram of the [Eu(mpa)₃(H₂O)] crystal

with double-gratings (1,200 gr/mm, 330 nm blaze) in the excitation monochromator and double-gratings (1,200 gr/mm, 500 nm blaze) in the emission monochromator. An ozone-free Xenon lamp of 450 W (Ushio) was used as a radiation source. The excitation spectra were obtained between 200 and 600 nm and they were corrected in real time according to the lamp intensity and the optical system of the excitation monochromator using a silicon diode as a reference. The emission spectra were carried out between 350 and 720 nm using the front face mode at 22.5°. All of them were corrected according to the optical system of the emission monochromator and the photomultiplier response (Hamamatsu R928P). The time resolved emission spectra were measured using a phosphorimeter system using time delay in a range from 0.015 ms to 0.13 ms, in order to get only the emissions from triplet states of the ligands. The emission decay curves were obtained with a pulsed 150 W Xenon lamp using a phosphorimeter. The absolute quantum yields were measured using a Quanta-φ (Horiba F-309) integrating sphere equipped with an optical-fibers bundle (NA=0.22 - Horiba-FL-3000/FM4-3000). X-Ray data were collected in a Bruker Apex with CCD detector and using Mo K_α radiation. The crystal structure was solved and refined using the software *SHELXL97* [23]. All estimated standard derivations (esds), except the esd in the dihedral angle between two l.s. planes,

**Fig. 4** Coordination polyhedron around europium(III) ion showing the tricapped trigonal prism geometry

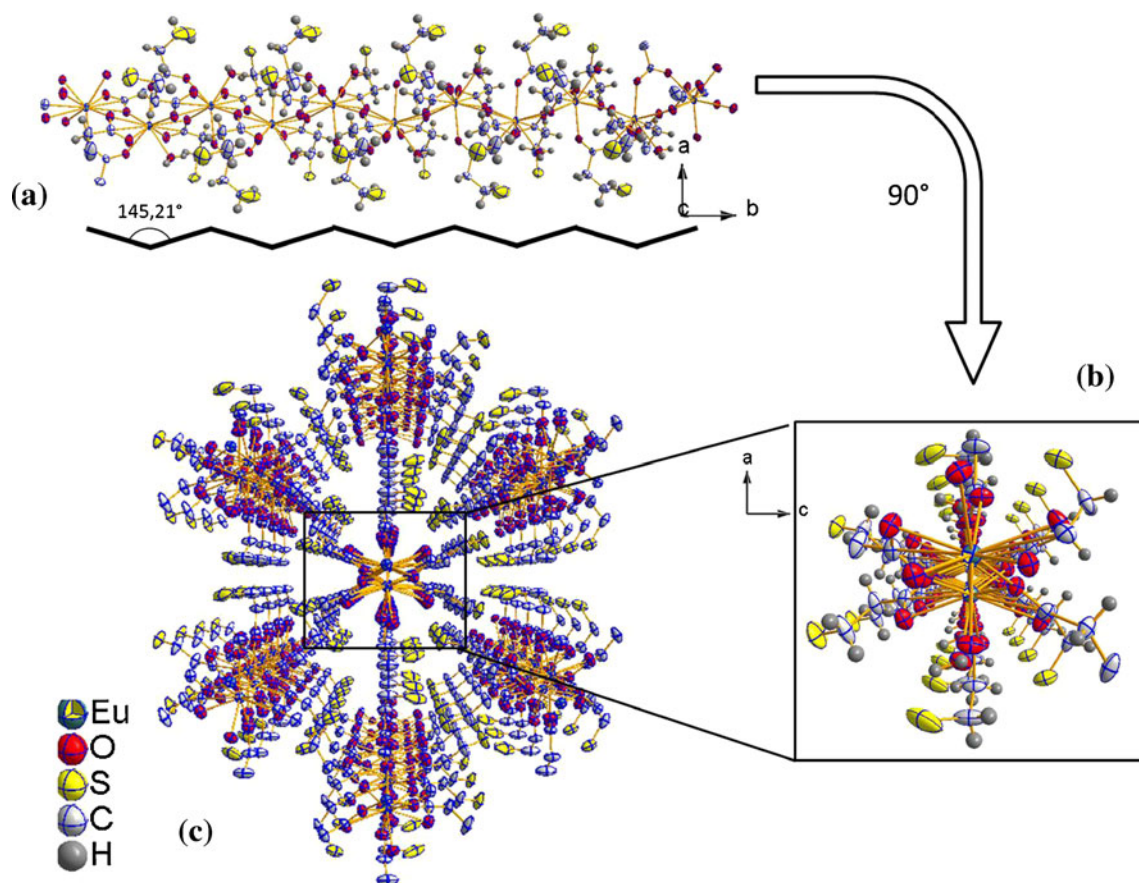


Fig. 5 Viewing of one chain of the $[\text{Eu}(\text{mpa})_3(\text{H}_2\text{O})]$ complex along c axis (a) and along b axis (b). Each one dimensional chain is surrounded by other six parallel one dimensional structures (c)

are estimated using the full covariance matrix. The cell esds are taken into account individually in the estimation of esds in distances, angles and torsion angles; correlations between esds in cell parameters are only used when they are defined by

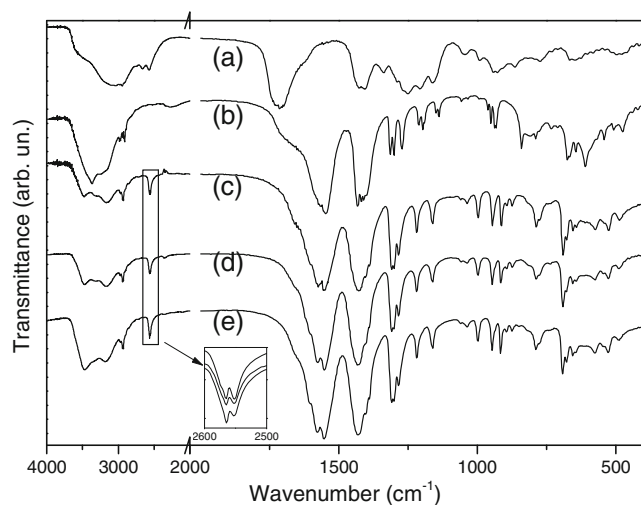


Fig. 6 FT-IR spectra of the Hmpa ligand (a), its ionic sodium salt (b) and the complexes: $[\text{Eu}(\text{mpa})_3(\text{H}_2\text{O})]$ (c), $[\text{Gd}(\text{mpa})_3(\text{H}_2\text{O})]$ (d) and $[\text{Tb}(\text{mpa})_3(\text{H}_2\text{O})]$ (e)

crystal symmetry. An approximate (isotropic) treatment of cell esds is used for estimating esds involving l.s. planes. Refinement of F^2 against all reflections. The weighted R-factor wR and goodness of fit S are based on F^2 , conventional R-factors R are based on F , with F set to zero for negative F^2 . The threshold expression of $F^2 > 2\sigma(F^2)$ is used only for calculating R-factors(gt) etc. and is not relevant to the choice of reflections for refinement. R-factors based on F^2 are statistically about twice as large as those based on F , and R-factors based on all data will be even larger.

Results and Discussion

The yields of the chemical reactions were: $[\text{Eu}(\text{mpa})_3(\text{H}_2\text{O})]$: 46 %; $[\text{Gd}(\text{mpa})_3(\text{H}_2\text{O})]$: 58 %; $[\text{Tb}(\text{mpa})_3(\text{H}_2\text{O})]$: 65 %. Elemental analysis of the $[\text{Eu}(\text{mpa})_3(\text{H}_2\text{O})]$ complex (%): calcd/obs for $\text{C}_9\text{H}_{17}\text{O}_7\text{S}_3\text{Eu}$: C, 22.28/21.91; H, 3.53/2.15; Eu, 31.32/32.33 %. Elemental analysis of the $[\text{Gd}(\text{mpa})_3(\text{H}_2\text{O})]$ complex (%): calcd/obs for $\text{C}_9\text{H}_{17}\text{O}_7\text{S}_3\text{Gd}$: C, 22.04/22.31; H, 3.49/2.07; Tb, 32.06/31.71 %. Elemental analysis of the $[\text{Tb}(\text{mpa})_3(\text{H}_2\text{O})]$ complex (%): calcd/obs for

Table 4 FT-IR bands (cm^{-1}) of the Hmpa, its ionic salt, Nampa, and $[\text{Ln}(\text{mpa})_3(\text{H}_2\text{O})]$ complexes

Samples	Hmpa	Nampa	$[\text{Eu}(\text{mpa})_3(\text{H}_2\text{O})]$	$[\text{Gd}(\text{mpa})_3(\text{H}_2\text{O})]$	$[\text{Tb}(\text{mpa})_3(\text{H}_2\text{O})]$
$\nu_{\text{O-H}}$	3080	3360	3470, 3160	3470, 3160	3470, 3190
$\nu_{\text{C-H}}$	2947	2921, 2912	2942, 2929	2942, 2929	2942, 2929
Acid dimer	2664, 2570	–	–	–	–
$\nu_{\text{S-H}}$	–	–	2565, 2552	2565, 2552	2565, 2552
$\nu_{\text{C=O}}$	1713	–	–	–	–
$\delta_{\text{C-O-H}}$ (in plane)	1415	–	–	–	–
$\nu_{\text{C-OH}}$	1250	–	–	–	–
$\delta_{\text{C-O-H}}$ (out of plane)	930	–	–	–	–
$\nu_{\text{as}}(\text{COO}^-)$	–	1547	1576, 1552	1576, 1550	1577, 1550
$\nu_{\text{s}}(\text{COO}^-)$	–	1417	1431	1430	1431
$\Delta\nu_{\text{COO}^-}$	–	130	145, 121	146, 120	146, 121
$\nu_{\text{as}}(\text{C-S})$	–	1314, 1301	1309, 1300	1309, 1300	1309, 1300

$\text{C}_9\text{H}_{17}\text{O}_7\text{S}_3\text{Tb}$: C, 21.96/22.00; H, 3.48/1.86; Tb, 32.29/31.61 %.

The thermogravimetric curves of the $[\text{Ln}(\text{mpa})_3(\text{H}_2\text{O})]$ complexes are quite similar, the curve of the $[\text{Eu}(\text{mpa})_3(\text{H}_2\text{O})]$ complex is shown in Fig. 2 and the TG/DTA curves of $[\text{Tb}(\text{mpa})_3(\text{H}_2\text{O})]$ and $[\text{Gd}(\text{mpa})_3(\text{H}_2\text{O})]$ ones are shown on electronic supplementary material (ESI – Figure S1). In general, just one endothermic event is observed at 78 °C and it may be attributed to the loss of a coordinated water molecule, corresponding to a mass loss varying from 3.4 up to 3.6 % for all complexes. The decomposition of the ligand occurs from 200 up to 700 °C. The final residual masses are between 42 and 45 % of the initial ones and the $[\text{Eu}(\text{mpa})_3(\text{H}_2\text{O})]$ residue was identified as europium oxysulfates, $\text{Ln}_2\text{O}_2\text{SO}_4$ by powder X-Ray diffraction of the residues (ESI – Figure S2).

Details of the crystal structure of the $[\text{Eu}(\text{mpa})_3(\text{H}_2\text{O})]$ complex are shown in Table 1. Bond distances and angles around the europium(III) ion are shown in Tables 2 and 3, respectively. The ORTEP diagram of the $[\text{Eu}(\text{mpa})_3(\text{H}_2\text{O})]$

complex is shown in Fig. 3 with labeled atoms. The structure was determined as an orthorhombic system and space group $Pbca$. Powder X-Ray diffractions of the obtained complexes (ESI – Figure S3) present the similar diffraction pattern for all complexes, indicating that they are isomorphic. Therefore only the crystallographic data of the $[\text{Eu}(\text{mpa})_3(\text{H}_2\text{O})]$ complex are shown and it will be used for the explanation of the photoluminescent data.

From the ORTEP diagram is possible to observe that the europium(III) ions are coordinated by nine oxygen ions where one of them belongs to the water molecule. The geometry of the first coordination sphere around the metallic ion forms a slightly distorted tricapped trigonal prism (Fig. 4), where the europium(III) ions are located in a point symmetry close to D_{3h} .

Each europium(III) ion is coordinated by six carboxylate groups. Two of them are bridging mode bonded, two as chelate mode and two carboxylate primarily bonded as a chelate also bond as bridging mode to a neighbor europium(III) ion. The

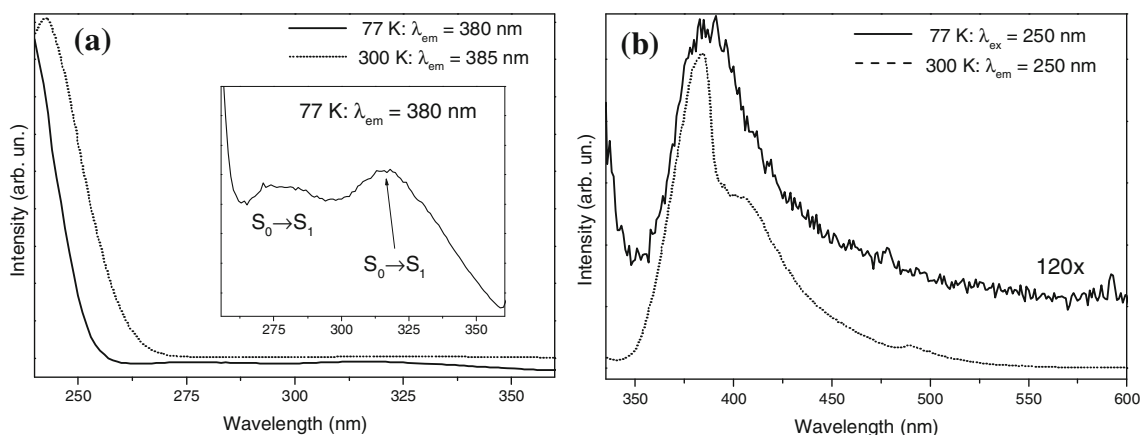


Fig. 7 Excitation (a) and emission (b) spectra of the $[\text{Gd}(\text{mpa})_3(\text{H}_2\text{O})]$ complex obtained at 77 and at 300 K. The inset shows a magnification of the excitation spectrum obtained at 77 K

Table 5 Judd-Ofelt intensity parameters (Ω), polarizability of bonding atoms (α), charge factor (g), emission lifetime (τ) of 5D_0 level, emission coefficients (A), ratio of the integrated areas of the $^5D_0 \rightarrow ^7F_0$ and $^5D_0 \rightarrow ^7F_2$ transitions (R_{02}), quantum efficiency (η) and absolute quantum yield (Φ) of $[\text{Eu}(\text{mpa})_3(\text{H}_2\text{O})]$ complex

	Ω_2 (10^{-20} cm^2)	Ω_4 (10^{-20} cm^2)	$\alpha(\text{COO}^-)$	$\alpha(\text{H}_2\text{O})$	$g(\text{COO}^-)$	$g(\text{H}_2\text{O})$	τ (ms)	A_{rad} (s^{-1})	A_{nrad} (s^{-1})	A_{tot} (s^{-1})	R_{02} (10^{-3})	η (%)	Φ (%)
Spectral values	6.05	5.43	–	–	–	–	0.80	312	938	1250	0.55	25	16
Crystal values	6.06	1.34	3.60	0.50	0.90	0.30	–	–	–	–	2.19	–	–

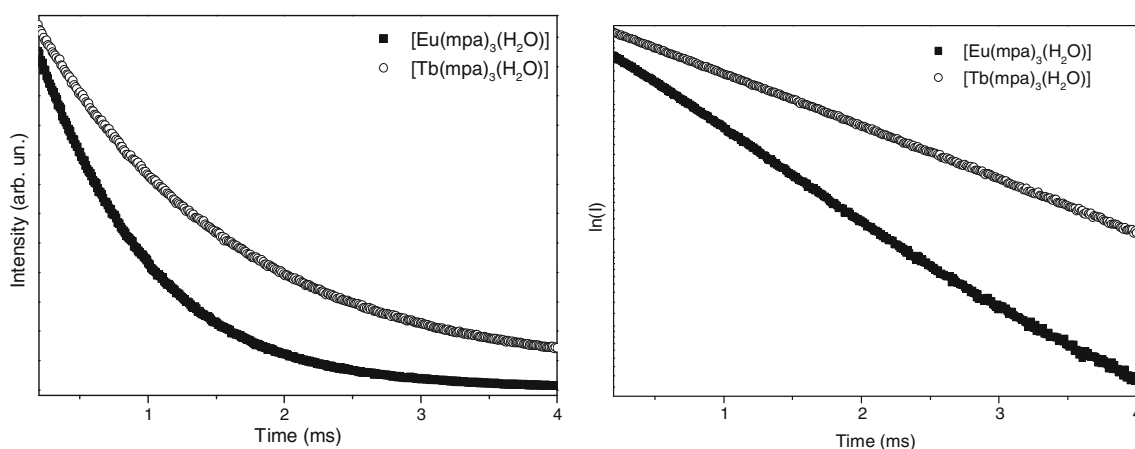
300 and at 77 K show just one intense band with maximum at energies higher than 250 nm. According to its energy and relative intensity this band may be attributed to a charge transfer band (CT). At 275 and 320 nm it is possible to observe two other bands much less intense than CT one (Fig. 7a-inset). The latter bands may be attributed to the excitation of the ligand from fundamental state S_0 to the excited states S_2 and S_1 , respectively. Under excitation at 250 nm the $[\text{Gd}(\text{mpa})_3(\text{H}_2\text{O})]$ complex has an emission band with maximum at 380 nm (Fig. 7b).

Time resolved emission spectra (Fig. 8) of the $[\text{Gd}(\text{mpa})_3(\text{H}_2\text{O})]$ was performed in order to attribute the broad emission band shown in Fig. 7b. These spectra were obtained at 77 K under excitation at 250 nm. From the time resolved emission spectra (Fig. 8) it is possible to distinguish two emission bands. At short delay time (0.015 ms), the first band, between 270 and 290 nm has a higher intensity than the second one observed between 350 and 450 nm. As a function of the delay time their intensities are inverted due to the difference between the emission lifetimes. Therefore, the data indicates that the bands may be attributed to the spin-allowed $S_1 \rightarrow S_0$ transition (fluorescence) and to the spin-forbidden $S_1 \rightarrow T_1$ transition (phosphorescence), respectively.

The excitation and emission spectra (Fig. 9) of the $[\text{Tb}(\text{mpa})_3(\text{H}_2\text{O})]$ obtained at 300 and at 77 K are quite

similar. The excitation spectra do not show any charge transfer band. That means that there is no energy transfer from the ligand to the excited level of the terbium(III) ion once the emission spectrum is monitored at the $^5D_4 \rightarrow ^7F_5$ transition. Both excitation and emission spectra of the $[\text{Tb}(\text{mpa})_3(\text{H}_2\text{O})]$ just show transitions attributed to $f-f$ intraconfigurational of terbium(III) ion due to the high energies of the ligand excited states. Terbium(III) complexes present low back-transfer rate when the energy of the triplet state of the ligand is higher than $22,300 \text{ cm}^{-1}$ [25, 26], that is about $1,850 \text{ cm}^{-1}$ higher than the 5D_4 emitting level of the terbium(III) ion. The absolute quantum yield of the $[\text{Tb}(\text{mpa})_3(\text{H}_2\text{O})]$ complex, excited at 369 nm ($^7F_6 \rightarrow ^5L_{10}$ transition) was determined as 19 %.

The excitation spectra of the $[\text{Eu}(\text{mpa})_3(\text{H}_2\text{O})]$ complex (Fig. 10) were obtained at 77 and 300 K exhibiting only narrow transitions that arises from $^7F_{0,1}$ levels of the europium(III) ion to its excited levels (Fig. 10). The emission spectra obtained at 77 and 300 K are quite similar showing no significant emission from ligand or from 5D_1 level. The number of Stark splitting of the europium(III) transitions that arises from 5D_0 emitting level is higher than expected for a D_{3h} symmetry. That happens because of the distortion of the symmetry site around the europium(III) ion the complex. The $^5D_0 \rightarrow ^7F_0$ transition (Fig. 10-inset), that should be absent for europium(III) ions in a D_{3h} symmetry is

**Fig. 11** Emission decay curves of the $[\text{Eu}(\text{mpa})_3(\text{H}_2\text{O})]$ and $[\text{Tb}(\text{mpa})_3(\text{H}_2\text{O})]$ complexes obtained at 300 K, monitoring the $^5D_0 \rightarrow ^7F_2$ transition of the europium(III) ion and the transition $^5D_4 \rightarrow ^7F_5$ of the

terbium(III) ion. The excitations were done at 396 nm and 352 nm for the $[\text{Eu}(\text{mpa})_3(\text{H}_2\text{O})]$ and $[\text{Tb}(\text{mpa})_3(\text{H}_2\text{O})]$ complexes, respectively

detected indicating the distortion around the D_{3h} symmetry. The ${}^5D_0 \rightarrow {}^7F_0$ transition is narrow (FWHM = 9.7 cm^{-1} , Fig. 10-inset) indicating a well distributed point symmetry around europium(III) ions through the sample.

The luminescent parameters of the $[\text{Eu}(\text{mpa})_3(\text{H}_2\text{O})]$ were measured from the spectral data and are shown on Table 5. Figure 11 exhibit the emission decay curves of the emitting levels, 5D_0 and 7F_5 of the europium(III) and terbium(III) ions, respectively. The curves were adjusted with a first order exponential decay function indicating that in both complexes the lanthanide ions are located in a similar chemical environment as identified by monocrystal X-ray diffraction (Fig. 3). Despite the water molecule in its coordination sphere, the europium(III) ion has a relatively long emission lifetime, 0.80 ms if compared with other europium(III) carboxylate coordination polymers²⁶ and even to europium(III) β -diketonate complexes. It happens probably due to the polymeric structure of the europium(III) complex that results in less vibronic coupling decreasing the non-radioactive rates from the 5D_0 emitting level. Due to the higher energy of the 5D_4 terbium(III) emitting level compared to the 5D_0 europium(III) emitting level, usually terbium(III) complexes have higher lifetime values, 1.42 ms for $[\text{Tb}(\text{mpa})_3(\text{H}_2\text{O})]$ complex.

To each observable ${}^5D_0 \rightarrow {}^7F_J$ transition in the emission spectrum it is associated a spontaneous emission coefficient $A_{0 \rightarrow J}$. ${}^5D_0 \rightarrow {}^7F_1$ transition is strictly allowed by magnetic dipole mechanism, its value is almost insensitive to changes in the chemical environment around europium(III) ion and it is assumed to be $A_{0 \rightarrow 1} = 50 \text{ s}^{-1}$. This transition is an internal reference and is used to calculate $A_{0 \rightarrow 2}$ and $A_{0 \rightarrow 4}$, as follows:

$$A_{0 \rightarrow J} = A_{0 \rightarrow 1} \left(\frac{\sigma_{0 \rightarrow 1}}{\sigma_{0 \rightarrow J}} \right) \left(\frac{I_{0 \rightarrow J}}{I_{0 \rightarrow 1}} \right)$$

where σ and I are, respectively, the barycenter and the integrated area under the transition at emission spectrum. Using experimental values of $A_{0 \rightarrow J}$, the experimental intensity parameters Ω_λ [27, 28] are calculated as

$$\Omega_\lambda = \frac{3hc^3 A_{0 \rightarrow J}}{4e^2 \omega^3 \chi \langle {}^7F_J \| U^\lambda \| {}^5D_0 \rangle^2}$$

where $\chi = n(n+2)^2/9$ is the Lorentz local field correction assuming refractive index $n = 1.5$, and $\langle {}^7F_J \| U^\lambda \| {}^5D_0 \rangle$ are the square reduced matrix elements, and are equal to 0.0032 for $J=2$ and 0.0023 for $J=4$.

The sum of all spontaneous emission coefficient gives the radiative rate A_{rad} . The sum of radiative A_{rad} and non-radiative A_{nrad} rates is called total rate A_{tot} , that is equal to the inverse of the lifetime τ of emitting state. So that the quantum efficiency is calculated as:

$$\eta = \frac{A_{rad}}{A_{rad} + A_{nrad}} = \frac{A_{rad}}{A_{tot}} = \tau A_{rad}$$

Judd-Ofelt intensity parameters as well as polarizability and charge factor of the bonding atoms [29] of the $[\text{Eu}(\text{mpa})_3(\text{H}_2\text{O})]$ complex were calculated from radiative rate obtained from the emission spectrum at 300 K and using the Judd-Ofelt theory (Table 5), respectively.

From Table 5 it is possible to notice the low values of decay rates (A) when compared to other complexes [30, 31], even hydrated carboxylates.²⁶ Despite the low A_{rad} value, the quantum efficiency of the $[\text{Eu}(\text{mpa})_3(\text{H}_2\text{O})]$ complex is not so low due to the relatively low value of the A_{tot} leading to a considerable value of the emission lifetime [32]. From the data (Table 5) one may observe the higher values of polarizability (α) than the charge factor (g) of the carboxylate group indicating the important contribution of the dynamic coupling mechanism on the intensity emission of the europium(III) ion in the complex.

Conclusion

A set of three lanthanide(III) 3-mercaptopropionate complexes were synthesized and characterized. The complexes are coordination polymers, where the units of each complex unit is linked together by carboxylate groups leading to an unidimensional and parallel chains that by chemical interactions form a tridimensional (3D) framework. Photoluminescent data of $[\text{Gd}(\text{mpa})_3(\text{H}_2\text{O})]$ complex suggest a high energy of the T_1 state ($28,000 \text{ cm}^{-1}$) that do not contribute to the energy transfer to europium(III) or terbium(III) on their respective complexes. However the structural rigidity of the complexes contributes to decrease non-radiative processes from emitting levels 5D_0 and 5D_4 of the europium(III) and terbium(III), respectively, as shown by the values of emission lifetime, quantum efficiency and absolute quantum yield.

Acknowledgment The authors acknowledge to Capes, CNPq and FAPESP for financial support. The authors also would like to thank Prof. C. H. Collins (IQ-UNICAMP, Campinas, Brazil) for English revision and the Laboratory of Advanced Optical Spectroscopy (LMEOA/IQ-UNICAMP/FAPESP grant # 2009/54066-7) for use of its equipment. This work is a contribution of the National Institute of Science and Technology in Complex Functional Materials (CNPq-MCT/Fapesp).

References

1. Niu SY, Yang GD, Zhang YL, Jin J, Ye L, Yang ZZ (2002) *J Mol Struc* 608:95
2. Kuchibhatla SVNT, Karakoti AS, Bera D, Seal S (2007) *Prog Mater Sci* 52:699
3. Stock N, Biswas S (2012) *Chem Rev* 112:933
4. Gagnon KJ, Perry HP, Clearfield A (2012) *Chem Rev* 112:1034
5. Czaja AU, Trukhan N, Müller U (2009) *Chem Soc Rev* 38:1284
6. Pan L, Adams KM, Hernandez HE, Wang X, Zheng C, Hattori Y, Kaneko K (2003) *J Am Chem Soc* 125:3062
7. Li J-R, Kuppler RJ, Zhou H-C (2009) *Chem Soc Rev* 38:1477
8. Kuppler RJ, Timmons DJ, Fang Q-R, Li J-R, Makal TA, Young MD, Yuan D, Zhao D, Zhuang W, Zhou H-C (2009) *Coord Chem Rev* 253:3042
9. Lee JY, Farha OK, Roberts J, Scheidt KA, Nguyen SBT, Hupp JT (2009) *Chem Soc Rev* 38:1450
10. Choi HJ, Lee TS, Suh MP (1999) *Angew Chem Int Ed* 38:1405
11. Ouchi A, Suzuki Y, Ohki Y, Koizumi Y (1988) *Coord Chem Rev* 92:29
12. Yu C-J, Tseng W-L (2008) *Langmuir* 24:12717
13. Devarajan S, Vimalan B, Sampath S (2004) *J Colloid Interface Sci* 278:126
14. Geraldo DA, Duran-Lara EF, Aguayo D, Cachau RE, Gonzalez-Nilo FD, Santos LS (2011) *Anal Bioanal Chem* 400:483
15. D'Souza S, Antunes E, Litwinski C, Nyokong T (2011) *J Photochem Photobiol A* 220:11
16. Chmura A, Szaciłowski K, Waksmundzka-Góra A, Stasicka Z (2006) *Nitric Oxide* 14:247
17. Gupta T, Dhar S, Nethaji M, Chakravarty AR (2004) *Dalton Trans* 1896
18. Kumar P, Baidya B, Chaturvedi SK, Khan RH, Manna D, Manna M (2011) *Inorg Chim Acta* 376:264
19. Su Y-T, Lan G-Y, Chen W-Y, Chang H-T (2010) *Anal Chem* 82:8566
20. Prasad P, Sasmal PK, Khan I, Kondaiah P, Kondaiah AR (2011) *Inorg Chim Acta* 372:79
21. Bear JL, Choppin GR, Quagliano JV (1963) *J Inorg Nucl Chem* 25:513
22. Choppin GR, Martinez-Perez LA (1968) *Inorg Chem* 7:2657
23. Sheldrick GM (2008) *Acta Crystallogr A Found Crystallogr* A64:112
24. Deacon GB, Phillips RJ (1980) *Coord Chem Rev* 33:227
25. Latva M, Takalo H, Mikkala V-M, Matachescu C, Rodriguez-Ubied JC, Kankare J (1997) *J Lumin* 75:149
26. Souza ER, Silva IGN, Teotonio EES, Felinto MCFC, Brito HF (2010) *J Lumin* 130:283
27. Judd BR (1962) *Phys Rev* 127:750
28. Ofelt GS (1962) *J Chem Phys* 37:511
29. Monteiro JHSK, Adati RD, Davolos MR, Vicenti JRM, Burrow RA (2011) *New J Chem* 35:1234
30. Sá GF, Malta OL, Donegá CM, Simas AM, Longo RL, Santa-Cruz PA, Silva EF Jr (2000) *Coord Chem Rev* 196:165
31. Souza ER, Zulato CHF, Mazali IO, Sigoli FA (2013) *J Fluor*. doi:10.1007/s10895-013-1219-5
32. Monteiro JHSK, Mazali IO, Sigoli FA (2011) *J Fluor* 21:2237